

0.214 T. Two types of stainless mesh grids [grid 1 (ϕ 6 cm, 10 mesh/inch) and grid 2 (doughnut shape, outside diameter: ϕ 6 cm, inside diameter: ϕ 3 cm, 30 mesh/inch)] are located at $z = -40$ cm and divide the source region from the experimental region. The ETG is easily formed by controlling the bias voltages applied to the grids. A tungsten (W) hot plate set at the end of the experimental region is heated by applying DC power $P_{\text{HP}} = 3$ kW and generates the low-temperature thermionic electrons ($T_e = 0.2$ eV), which works as an electron emitter. Since the electron emitter is concentrically segmented into two sections, a radial profile of the space potential is controllable by applying different bias voltages between central (V_{ec1}) and peripheral (V_{ec2}) sections of the electron emitter. The low-temperature thermionic electrons compensate the density gradient of the ECR plasma penetrating the grid 2. Therefore, the large ETG is formed in the experimental region keeping the radial density profile uniform. A Langmuir probe is used to measure radial profiles of plasma parameters at $z = 0$ cm in the experimental region [7].

3. Experimental Results and Discussion

Using this novel plasma synthesis method superimposing the high-temperature electrons on the low-temperature electrons with spatially control, the ETG can be formed in the experimental region. Figure 2 shows the electron temperature as functions of the bias voltages of (a) grid 1 (V_{g1}) and (b) grid 2 (V_{g2}) in the radially central ($r = 0$ cm) and peripheral ($r = 2$ cm) regions for $V_{\text{ec1}} = V_{\text{ec2}} = 0$ V, $P_{\mu} = 30$ W. When V_{g2} is decreased, the electron temperature only in the peripheral region rapidly decreases, while the electron temperature in the central region is almost constant. Therefore, the electron temperature difference between the central and peripheral regions, i.e., the ETG, is easily formed by controlling V_{g2} with an appropriate adjustment to V_{g1} .

On the other hand, the decrease in V_{g1} causes the decrease in the electron temperature in both the central and peripheral regions. However, when V_{g1} is less than 0 V, the decrease in the electron temperature in the central region ($r = 0$ cm) is observed to mitigate in contrast to that in the peripheral region. It is considered that the ions of the ECR plasma are accelerated and collide with the negatively biased grid 1, and as a result, secondary electrons are generated from the grid 1. The secondary electrons are accelerated by the potential difference between grid 1 and plasma potential in the experimental region, and then, the accelerated high energy electrons are thermalized by collision with neutral gas or low temperature electrons, resulting in the mitigation of the decrease in the electron temperature in the central region. On the other hand, the secondary electrons are not accelerated in the peripheral region because the grid 2 prevents the electrons from penetrating into the experimental region. When V_{g1} is less than -20 V, the ions are difficult to collide with grid 1 because the ions

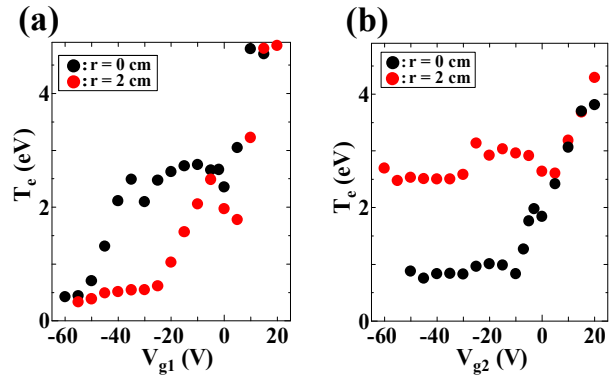


Fig. 2. Electron temperature (T_e) in the central and peripheral regions as functions of (a) V_{g1} for floated V_{g2} , and (b) V_{g2} for floated V_{g1} for $V_{\text{ec1}} = V_{\text{ec2}} = 0$ V, $P_{\mu} = 30$ W.

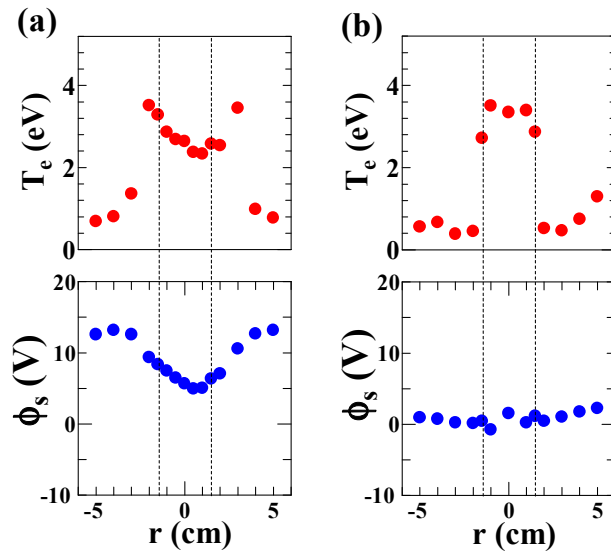


Fig. 3. Radial profiles of electron temperature T_e and space potential ϕ_s for (a) $V_{g2} = 10$ V and (b) $V_{g2} = -30$ V. $V_{g1} = -10$ V, $V_{\text{ec1}} = V_{\text{ec2}} = 0$ V, and $P_{\mu} = 30$ W. Dotted lines indicate the boundary between grid 1 and grid 2.

with higher energy have smaller Coulomb collision frequency.

Figure 3 shows the radial profiles of the electron temperature (T_e) and the space potential (ϕ_s) for (a) $V_{g2} = 10$ V and (b) $V_{g2} = -30$ V, where $V_{g1} = -10$ V. In the case of $V_{g2} = 10$ V, the radial profile of the electron temperature is almost flat at the boundary region between grid 1 and grid 2. When V_{g2} decreases to -30 V, on the other hand, the high temperature electrons of the ECR plasma in the peripheral region are reflected back to the source region, and therefore, the electron temperature only in the peripheral region becomes small, resulting in the formation of the steep ETG around $r = -1.5$ cm.

The space potential is almost flat, even when the ETG is formed [Fig. 3(b)], which is caused by the same bias voltages (V_{ce1} and V_{ce2}) applied to the electron emitters. However, the large positive bias voltage such as $V_{g2} = 10$ V affects the space potential as shown in Fig. 3(a). Here, the radial profiles of the electron density are relatively uniform even when the ETG is formed.

Figure 4 gives frequency spectra of the fluctuation of the electron saturation current (I_{es}) with (a) high and (b) low frequencies under the same conditions as in Fig. 3. In the case of the high frequency range [Fig. 4(a)], the fluctuation is more strongly excited when the ETG is formed for $V_{g2} = -30$ V. Furthermore, the low frequency fluctuation around 3~4 kHz is also enhanced when the ETG is formed. Since the ETG is not considered to directly affect the low frequency fluctuation, the ETG can enhance the low frequency fluctuation through the coupling with the high frequency ETG mode.

Figure 5 presents the normalized peak amplitudes $\tilde{I}_{es} / \bar{I}_{es}$ of fluctuations as a function of V_{g2} (\bar{I}_{es} : time averaged value of I_{es}) for (a) high-frequency (5 MHz) and (b) low-frequency (about 3 kHz) fluctuations. The peak amplitude of the high-frequency fluctuation gradually increases with a decrease in V_{g2} in the same way as the strength of the ETG which is estimated from Fig. 2(b). Therefore, this fluctuation is believed to be the ETG mode. On the other hand, the peak amplitude of the low frequency fluctuation also increases with a decrease in V_{g2} . This phenomenon is explained by the coupling between the high and low frequency fluctuations, namely, the ETG mode can enhance the low frequency fluctuation.

In order to investigate the suppression mechanism of the ETG mode by the $E \times B$ velocity shear, we control the bias voltage of the central electron emitter V_{ce2} to generate the local radial electric field in the magnetized plasma. Figure 6 gives the normalized peak amplitudes $\tilde{I}_{es} / \bar{I}_{es}$ of the fluctuations as a function of V_{ce2} for (a) high-frequency (5 MHz) and (b) low-frequency (about 3 kHz) fluctuations. Here, since V_{ce1} is 1 V, the $E \times B$ velocity shear is not formed for $V_{ce2} = 1$ V, and its strength increases with increasing or decreasing V_{ce2} from 1 V.

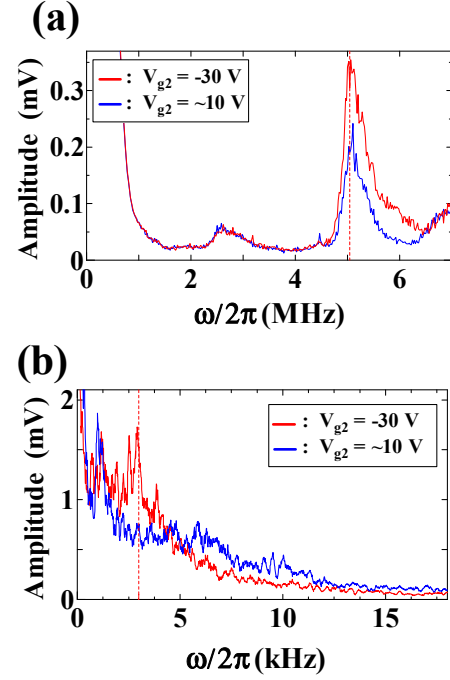


Fig. 4. Frequency spectra of the fluctuation of electron saturation current I_{es} with (a) high and (b) low frequencies for $V_{g1} = -10$ V, $V_{ce1} = V_{ce2} = 0$ V, and $P_{\mu} = 30$ W at $r = -1.5$ cm.

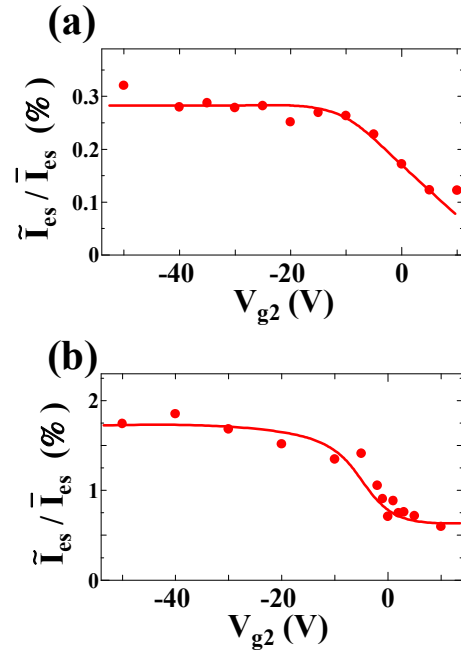


Fig. 5. Normalized peak amplitudes $\tilde{I}_{es} / \bar{I}_{es}$ of fluctuations with low and high frequencies as a function of V_{g2} (\bar{I}_{es} : time averaged value of I_{es}) for (a) high-frequency (5 MHz) and (b) low-frequency (about 3 kHz) fluctuation.

The peak amplitude of the high frequency ETG mode is found to gradually decrease with an increase in the $E \times B$ velocity shear strength, which means that the ETG mode could be suppressed by the $E \times B$ velocity shear. On the other hand, the peak amplitude of the low frequency fluctuation becomes large, when the strength of the $E \times B$ velocity shear increases. Therefore, the low frequency fluctuation is considered to be the Kelvin-Helmholtz (K-H) instability. Since the peak amplitude of this K-H instability in the presence of the ETG is larger than that in the absence of the ETG, it is expected that the K-H instability is enhanced by the coupling with the ETG mode.

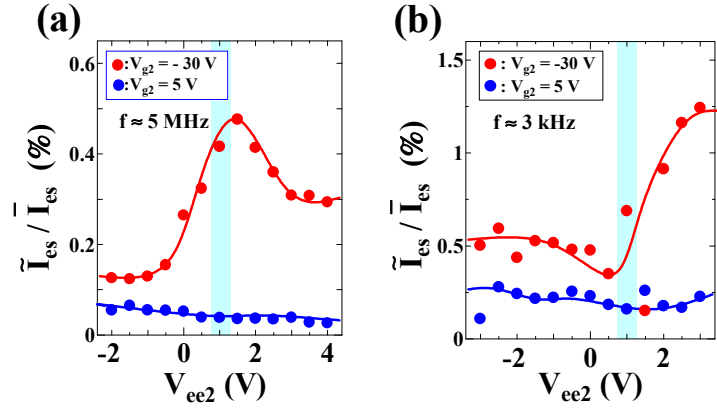


Fig. 6. Normalized amplitudes $\tilde{I}_{es} / \bar{I}_{es}$ of fluctuation with (a) high and (b) low frequencies as a function of V_{ee2} for $V_{ce1} = 1$ V, $V_{g1} = -10$ V, and $P_{\mu} = 30$ W at $r = -1.5$ cm.

4. Conclusion

A novel plasma synthesis method superimposing the high-temperature electrons on the low-temperature electrons has developed to form and control the ETG in a magnetized plasma. The formed ETG is found to excite the high-frequency fluctuation, i.e., ETG mode, and also, to enhance a low-frequency fluctuation originally caused by the $E \times B$ velocity shears. Furthermore, it is clarified that the strong $E \times B$ velocity shear suppresses the ETG mode experimentally.

5. Acknowledgments

The authors are indebted to H. Ishida for his technical assistance. We also express our gratitude to Professor K. Ito, Prof. S. Inagaki, Dr. K. Kamataki, and Dr. M. Nakata for their useful comments and discussion. This work was supported by a Grant-in-Aid for Scientific Research from the Ministry of Education, Culture, Sports, Science and Technology, Japan.

6. References

1. C. Holland and P. H. Diamond, "Electromagnetic secondary instabilities in electron temperature gradient turbulence", *Phys. Plasmas*, **9**, 2002, pp. 3857-3866.
2. F. Jenko, W. Dorland, and G. W. Hammett, "Critical gradient formula for toroidal electron temperature gradient modes", *Phys. Plasmas*, **8**, 2001, pp. 4096-4104.
3. Z. Gao, J.Q. Dong, and H. Sanuki, "Effects of flow shear on temperature gradient driven short wavelength modes", *Phys. Plasmas*, **11**, 2004, pp. 3053-3059.
4. A. Hirose, "Effects of charge non-neutrality and finite β on the electron temperature gradient mode", *Phys. Plasmas*, **10**, 2003, pp. 4567-4569.
5. Y. Idomura, S. Tokuda, and M. Wakatani, "Gyrokinetic theory of slab ion temperature gradient mode in negative shear tokamaks", *Phys. Plasmas*, **6**, 1999, pp. 4658-4671.
6. E. Asp, J. -H. Kim, W. Horton, L. Porte, S. Alberti, A. Karpushov, Y. Martin, O. Sauter, G. Turri, and the TCV TEAM, "Electron thermal transport analysis in Tokamak à Configuration Variable", *Phys. Plasmas*, **15**, 2008, pp. 082317-1-16.
7. C. Moon, T. Kaneko, S. Tamura, and R. Hatakeyama, "Control of electron temperature and space potential gradients by superposition of thermionic electrons on electron cyclotron resonance plasmas", *Rev. Sci. Instrum.*, **81**, 2010, pp. 053506-1-4.